Mission Analysis of Spinning Systems for Transfers from Low Orbits to Geostationary

E. C. Lorenzini[*] and M. L. Cosmo[*]
Harvard–Smithsonian Center for Astrophysics, Cambridge, Massachusetts 02138
M. Kaiser[†]
Technical University of Munich, 8000 Munich, Germany
M. E. Bangham[‡] and D. J. Vonderwell[‡]
The Boeing Company, Huntsville, Alabama 35824
and
L. Johnson[§]
NASA Marshall Space Flight Center, Huntsville, Alabama 35812

An analysis of the use of spaceborne spinning tethers for a reusable system to transfer payloads with a mass up to 4000 kg from low orbits to geostationary is presented. Results indicate that a two-stage system is lighter than a single-stage tethered system with present-day tether materials. A first stage in low orbit and a second stage in medium Earth orbit provide the required velocity increments for injecting the payload into geotransfer orbit with the final orbit circularization provided by the satellite kick motor. The orbits of the stages are resonant in order to provide periodic encounters and are optimized with the goal of reducing the overall system mass. The close-approach dynamics between the second stage and the payload released from the first stage is simulated to demonstrate the salient features of the rendezvous process. A total of 10 transfers over two years of operation without refueling is adopted for computing the propellant needed to reboost the stages. A preliminary analysis leads to the conclusion that a two-stage tethered system is more competitive, on a mass basis, than a chemical upper stage after two transfers.

Nomenclature

a	= semimajor axis
E	= orbital energy
e	= orbital eccentricity or exponential function
f	= safety factor
g	= Earth's gravity acceleration
H	= altitude above ground
I_{sp}	= specific impulse
J_2	= second zonal harmonic of the Earth's gravity field
L	= overall tether length
L_{ij}	= distance along tether
l_{ij}	= distance along tether
M	= ratio between transfer orbit and first-stage orbital periods
m	= mass
N	= ratio between second-stage and first-stage orbital periods
P	= orbital period
r	= geocentric radius
V	= velocity
ΔV	= velocity increment
μ	= Earth's gravitational constant
ρ	= mass density
σ	= ultimate strength
τ	= tether/platform mass ratio
χ	= payload/platform mass ratio
ω	= angular speed, rad/s

Subscripts

a	= apogee
c	= critical
circ	= circularization
min	= minimum value
p	= perigee
pay	= payload
prop	= propellant
tet	= tether
tip	= tether tip
1	= first stage i or platform j
2	= second stage i or payload j

Introduction

THE scope of this paper is to conduct a system-level mission analysis of a reusable, spinning tethered system for transferring payloads from low Earth orbit (LEO) to geostationary orbit (GEO). The analysis focuses on the orbital dynamics and the minimization of the overall mass of the transfer system. The system conceptual design and preliminary data about its subsystems are discussed in Ref. 1. The motivation for this study is that the projected traffic to GEO is expected to increase[2] during the next few decades and that the cost of delivering payload from the Earth surface to LEO is projected to decrease thanks to the introduction of reusable launching vehicles (RLV). A comparable reduction in upper stages cost must occur to deliver payloads to GEO at a fraction of today's expenses.

Consequently, studies for alternative means of transportation from LEO to GEO have been carried out with the aim of reducing substantially the cost per kilogram in transferring to GEO. Tethers are possible candidates to accomplish this goal because spinning tethers are excellent storage devices of kinetic energy and capable of imparting large velocity increments to the payload attached to the tether tip. A tethered system for transferring payload from LEO to GEO with a single stage was first proposed by Bekey and Penzo.[3] This work capitalizes on that idea and pushes it a few steps forward.

Spinning tethers are used to impart the desired velocity increments ΔV to the payload to be transferred. Each spinning system has a counter platform (or service module) on the opposite side of the tether. The spinning system acts as a giant momentum wheel, that is, for each ΔV imparted to the payload there is a ΔV, proportional to the spinning stage mass ratios, imparted to the platform
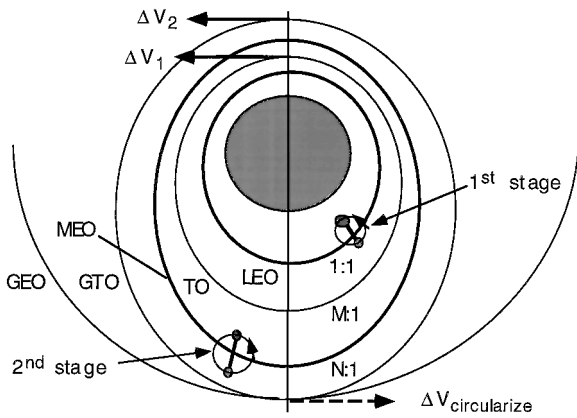
Fig. 1   Orbital sketch of two-stage tethered system for transferring satellites from LEO to GEO.

and the tether attached to it. After release, the payload is injected into a higher orbit, and the platform is injected into a lower orbit that depends on the mass distribution of the spinning system.

The transfer from LEO to geotransfer orbit (GTO) can be accomplished through a single ΔV of about 2.4 km/s (from a 300-km circular orbit) provided by a single-stage tethered system or through two smaller ΔV provided by a two-stage tethered system. This latter configuration is lighter with present-day tether technology (as explained later). A two-stage tethered system involves two facilities permanently in orbit (Fig. 1): a spinning facility in LEO and another one in medium Earth orbit (MEO) with a perigee close to the LEO facility. The two stages are in equatorial orbits. The payload is first boosted with a velocity increment ΔV_1 to MEO from the LEO facility. The payload is then captured (with zero relative velocity) at perigee by the MEO facility, and at a subsequent perigee passage, it is injected into GTO by means of the velocity increment ΔV_2. In this study, the circularization ΔV from GTO to GEO is considered to be provided by the kick motor of the payload. After payload delivery the two orbital platforms are reboosted by high specific impulse electrical thrusters. The masses of the payloads to be handled by the tethered transfer system are assumed in the range 907–4082 kg (2000–9000 lb) that, according to present projections,[2] will constitute almost 80% of the traffic to GEO in the future.

Orbital Transfer with Tethers

If we refer the system dynamics to a local vertical–local horizontal (LV–LH) reference frame attached to the system c.m., then tethers can be classified according to their motion with respect to LV–LH as hanging, swinging, or spinning much as a pendulum in a gravity field (a tethered system in orbit is in fact a gravity-gradient pendulum). Clearly, for a given tether length, spinning tethers can impart the highest ΔV to the payload. If we call ΔH the radial separation between the two tip masses half an orbit after release and L the tether length, the following simple rules[4] apply (Fig. 2) for hanging, swinging, and spinning tethers, respectively:

$$\Delta V \approx 7L, \qquad 7L < \Delta H < 14L, \qquad \Delta H > 14L \qquad (1)$$

Given that the required ΔH (or alternatively ΔV) are very high for a transfer from LEO to GTO, spinning tethers are the only practical solution for achieving the desired goal with tethers of moderate lengths.

Tethers can have a constant cross section (cylindrical tethers) or a varying cross section (tapered tethers). The maximum velocity that a cylindrical spinning tether can sustain (the so-called tether characteristic velocity), without any payload attached to its end, is limited by its material properties and can be written as follows:

$$V_c = \sqrt{2\sigma/f\rho} \qquad (2)$$

The ΔV that a cylindrical tether can provide, therefore, is bounded. For example, the best tether material now available, Spectra 2000, has a $V_c = 2.6$ km/s ($\sigma = 3.25 \times 10^9$ N/m² and $\rho = 970$ kg/m³)
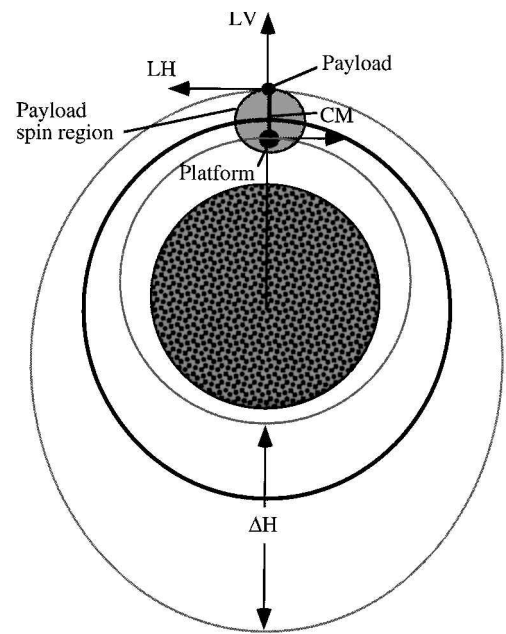

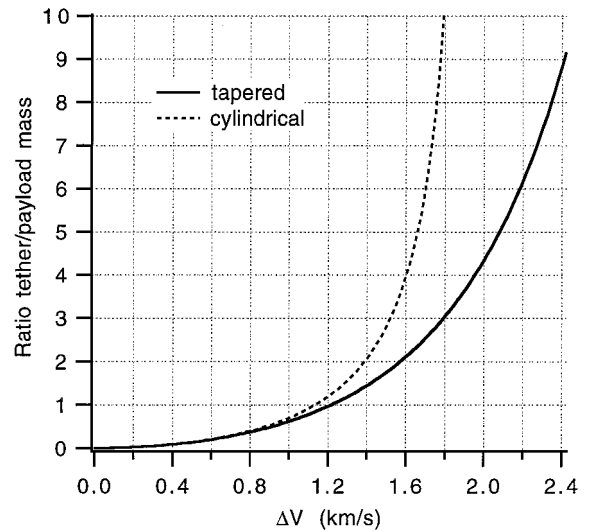**Fig. 2   Orbits after cut at LV of a spinning tether.**

Fig. 3   Tether/payload mass ratio for cylindrical and tapered tethers of Spectra 2000 and safety factor = 1.75.

with a safety factor of 1 (no safety margin) and $V_c = 1.96$ km/s with a safety factor of 1.75 as recommended for a fail-safe tether.[5]

Because the maximum stress is at the hub of a spinning tether, the tether can be tapered, thus saving tether mass and removing the limitation on the maximum sustainable ΔV. The mass of an optimally (i.e., with a constant stress distribution) tapered tether can be written as a function of the tip mass (payload) m_{pay} as follows[6,7]:

$$m_{tet}/m_{pay} = \sqrt{\pi}(V/V_c)\exp\left(V^2\big/ V_c^2\right)\mathrm{erf}(V/V_c) \qquad (3)$$

where V is the tip velocity and erf() is the error function. Figure 3 shows the tether/payload mass ratio for a cylindrical and a tapered tether of the same material (Spectra 2000) and a safety factor equal to 1.75. In conclusion, a tapered tether is lighter than a cylindrical tether for $\Delta V > 1$ km/s, and, moreover, the ΔV that a tapered tether can impart is not bounded by the strength to density ratio of the material. For $\Delta V < 1$ km/s, the masses of Spectra 2000 cylindrical and tapered tethers are almost equal.

Staging

In a zero-order approximation, a spinning tether can be compared to a rocket by comparing the tether mass needed to provide
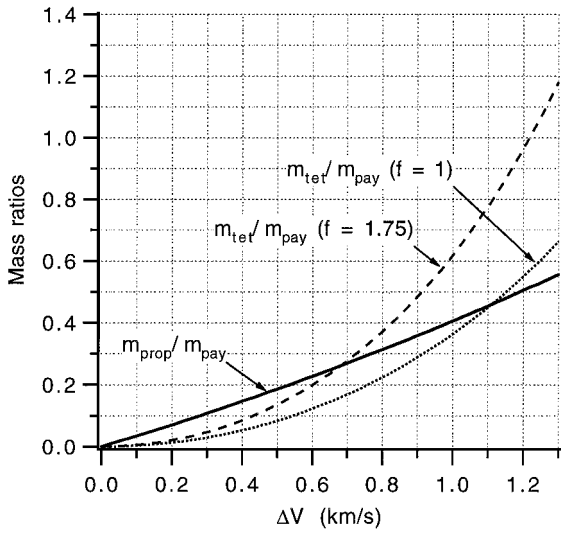
Fig. 4 Ratios of tether and propellant mass to payload mass vs ΔV for Spectra 2000 tethers (f = load safety factor) and 300-s, specific impulse propellant.

the desired ΔV imparted to the payload and the propellant mass required to accomplish the same task. The ratio of the propellant mass m_{prop} over the payload mass m_{pay} is readily computed by the rocket equation

$$m_{prop}/m_{pay} = [\exp(V/I_{sp}g) - 1] \tag{4}$$

$I_{sp}g$, in Eq. (4), is simply the gas ejection velocity from the rocket nozzle, that, for a hydrazine system and several solid propellants normally used in upper stages, is about 3 km/s.

Clearly, many other considerations apply to the comparison of tether systems vs chemical propulsion (as shown later in this paper) among which the most important is that a tethered system is reusable whereas a chemical system is not. Nevertheless, Fig. 4 gives a good indication of the ΔV range in which a spinning tether transportation system should operate with the best tether material presently available.

Because a ΔV of 2.4 km/s is required to inject a payload into GTO, if a single-stage tethered system (with present-day tether materials) were to be used, the mass of the tether would be about nine times the payload mass whereas the comparable propellant (hydrazine) mass would be less than two times the payload mass. In other words, based on this highly simplified analysis, it would take about five launches for a single-stage tethered system to become competitive. However, this preliminary conclusion can be improved dramatically by analyzing a two-stage system that, by splitting the ΔV into two smaller components, utilizes the tethers at their best with present-day tether materials.

Orbital Mechanics

Introductory Remarks

In a two-stage tethered system, the first-stage tether rotates with angular rate ω_1 and orbits in a LEO defined by its perigee r_{1p} and apogee radius r_{1a}. The second stage, which rotates with an angular rate ω_2, is at MEO between LEO and GEO. Both orbits lie on the equatorial plane. The orbit of the second stage is also elliptical to provide a velocity match at perigee, at the capture of the satellite released from the first stage, between the tether tip velocity and the incoming satellite that follows the transfer orbit (TO). For best efficiency, ΔV are imparted at perigee where the energy produced by a given ΔV is maximum because the orbital velocity is maximum.

An important consideration is the synchronicity[5] between the LEO, the TO after release from the first stage, and the MEO of the second stage. Synchronicity between the orbits of the first and the second stage provides periodic encounters between the two stages once the lines of apses of the two orbits are close to being aligned. Synchronicity between the orbit of the second stage (MEO) and

the transfer orbit of the payload (TO) provides multiple capture opportunities if the first capture attempt is missed.

Orbital Perturbations

The orbital model utilized in the following computations is simplified as it adopts a spherical gravity field and neglects environmental perturbations. Whereas the latter assumption is adequate considering the orbits involved (see also Ref. 1), the former assumption must be qualified because of the role played by the Earth's oblateness (i.e., the J_2 gravity component). Specifically, because the stages lie on the equatorial plane the differential precession of the first- and second-stage lines of apses is different from zero. The realignment frequency of the lines of apses determines the maximum launching frequency at minimum energy, that is, a transfer whereby a negligible amount of energy is spent to correct for mismatches of the apsidal lines. The apsidal realignment period of the two-stage orbital configuration analyzed in this paper is 72 days and, consequently, the ideal maximum launching frequency is 5 launches per year. Additional comments on techniques for compensating possible mismatches between the orbit of the stages are dealt with in the section "Rendezvous and Capture" of this paper.

Orbital Model

The orbital periods P of the TO and MEO can be expressed as follows:

$$P_{TO} = MP_1 \tag{5a}$$

$$P_2 = NP_1 \tag{5b}$$

The orbital period ratios M and N do not necessarily have to be integer numbers for having periodic encounters but rather rational numbers, that is, M and N, must satisfy the following equation to provide periodic encounters, with K and J being integer numbers:

$$M/N = K/J \tag{6}$$

The satellite is first released by the first stage at perigee, that, in an ideal situation, should have the same orbital anomaly of the perigee of the second stage. If the satellite is released when the tether crosses the local vertical, the perigee of TO is also at the point of release. After a time $T_{rev} = NKP_1$ (revisit time) the satellite passes through the perigee of TO when the second stage is close to the perigee of MEO (i.e., there are multiple recapture opportunities).

In Fig. 5, $L_1 = L_{11} + L_{12} = l_{11} + l_{12}$ and $L_2 = L_{21} + L_{22} = l_{21} + l_{22}$ are the overall lengths of the first- and second-stage tethers. The variables L are the distances from the platform and the payload to the stage c.m. with the payload attached, whereas the variables l are the distances to the c.m.* without the payload attached.

After defining $\chi_i = m_{pay}/m_{plat-i}$ and $\tau_i = m_{tet-i}/m_{plat-i}$, where $i = 1$ and 2 for the first and second stage, respectively, we obtain for the distances to c.m. the following:

$$L_{i1} = \frac{2\chi_i + \tau_i}{2(1 + \chi_i + \tau_i)} L_i, \qquad L_{i2} = \frac{2 + \tau_i}{2(1 + \chi_i + \tau_i)} L_i$$
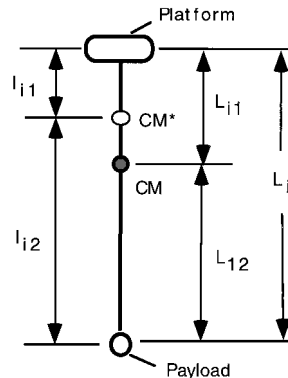
$$i = 1, 2 \tag{7a}$$

Fig. 5 Geometry of tethered stage.

and for the distances to c.m.[*]

$$l_{i1} = \frac{\tau_i}{2(1 + \tau_i)} L_i, \qquad l_{i2} = \frac{2 + \tau_i}{2(1 + \tau_i)} L_i, \qquad i = 1, 2 \quad (7b)$$

The orbital velocity of the first-stage c.m. at perigee is

$$V_{p1} = \sqrt{\mu / r_{p1}} \sqrt{1 + e_1} \qquad (8)$$

where r_{p1} is the perigee radius and e_1 is the orbital eccentricity. The velocities at perigee of the second-stage c.m.[*] (before satellite capture) and of the satellite on its TO after release from the first stage are, respectively,

$$V_{p2} = \sqrt{\frac{\mu}{r_{p1}}} \sqrt{\frac{2}{(L_{12} + l_{22})/r_{p1} + 1} - (1 - e_1)N^{-\frac{2}{3}}} \quad (9a)$$

$$V_{pTO} = \sqrt{\frac{\mu}{r_{p1}}} \sqrt{\frac{2}{L_{12}/r_{p1} + 1} - (1 - e_1)M^{-\frac{2}{3}}} \qquad (9b)$$

Because $\omega_1 = (1/L_{12})(V_{pTO} - V_{p1})$ and $\omega_2 = (1/l_{22})(V_{p2} - V_{pTO})$, the rotational rates of the two stages are as follows:

$$\omega_1 = \frac{1}{L_{12}} \sqrt{\frac{\mu}{r_{p1}}} \left[\sqrt{\frac{2}{L_{12}/r_{p1} + 1} - (1 - e_1)M^{-\frac{2}{3}}} - \sqrt{1 + e_1} \right]$$

(10a)

$$\omega_2 = \frac{1}{l_{22}} \sqrt{\frac{\mu}{r_{p1}}} \left[\sqrt{\frac{2}{(L_{12} + l_{22})/r_{p1} + 1} - (1 - e_1)N^{-\frac{2}{3}}} \right.$$

$$\left. - \sqrt{\frac{2}{L_{12}/r_{p1} + 1} - (1 - e_1)M^{-\frac{2}{3}}} \right]$$

(10b)

The velocity increment ΔV_1 imparted by the first stage and the perigee velocity of the satellite in the TO are

$$\Delta V_1 = \omega_1 L_{12} \qquad (11a)$$

$$V_{pTO} = V_{p1} + \Delta V_1 \qquad (11b)$$

The perigee radius of the satellite in TO is

$$r_{pTO} = r_{p1} + L_{12} \qquad (11c)$$

The second stage captures the incoming satellite at a velocity equal to $V_{p2} - \omega_2 L_{22}$ and accelerates it to a velocity $V_{p2} + \omega_2 L_{22}$, thereby producing a velocity increment $\Delta V_2 = 2\omega_2 L_{22} = 2V_{tip-2}$ whereas Eq. (11a) yields $\Delta V_1 = V_{tip-1}$ for the first stage.

The ΔV imparted by the second stage and the perigee velocity of the satellite in GTO after release are

$$\Delta V_2 = 2\omega_2 L_{22} \qquad (12a)$$

$$V_{pGTO} = V_{pTO} + \Delta V_2 \qquad (12b)$$

and the GTO perigee radius is

$$r_{pGTO} = r_{p1} + L_{12} + 2L_{22} \qquad (12c)$$

At the apogee of the GTO, the orbit must be circularized with an additional velocity increment ΔV_{circ} as follows:

$$\Delta V_{circ} = \sqrt{\mu / r_{aGTO}} - V_{aGTO} \qquad (13)$$

where r_{aGTO} and V_{aGTO} can be readily obtained from conservation of energy and angular momentum as shown later. The circularization velocity increment is assumed to be provided by the apogee kick motor of the satellite.

Minimization of System Mass

The orbital design (defined, among others, by the parameters M, N, and e_1) and the mass distribution of the system (defined by the parameters $\chi_1, \chi_2, \tau_1, \tau_2$) are derived in this section with the goal of minimizing the overall mass of the system.

Orbital constraint equations and tether-strength constraint equations are used to compute the preceding parameters. For a successful delivery of the payload into GTO, the apogee radius of the satellite orbit after release from the second stage must be equal to the geostationary radius. From conservation of energy and angular momentum we can readily obtain the apogee radius and velocity of the satellite after release as follows:

$$r_{aGTO} = \frac{r_{pGTO}}{\dfrac{2\mu}{r_{pGTO} V_{pGTO}^2} - 1} \qquad (14a)$$

$$V_{aGTO} = V_{pGTO}(r_{pGTO} / r_{aGTO}) \qquad (14b)$$

Algebraic manipulation of Eq. (14a) leads to the following orbital-constraint equation:

$$2\left\{ \sqrt{2 - (1 - e_1)M^{-\frac{2}{3}}} + 2\frac{1 + \tau_2}{1 + \chi_2 + \tau_2} \left(\sqrt{2 - (1 - e_1)N^{-\frac{2}{3}}} \right.\right.$$

$$\left.\left. - \sqrt{2 - (1 - e_1)M^{-\frac{2}{3}}} \right) \right\}^{-2} - \frac{r_{p1}}{r_{aGTO}} - 1 \approx 0 \qquad (15)$$

which is valid, with good approximation, for L_{12} and $l_{22} \ll r_{p1}$.

The tether-strength constraint equation is obtained by simply imposing that the tether at c.m. withstands the mechanical load generated by the satellite and the tether spinning with tip velocity V_{tip-2}. The tip velocities and not the ΔV determine the structural strength of the stages. Consequently, the first-stage tether must be designed to withstand a tip velocity $V_{tip-1} = \Delta V_1$ and the second-stage tether a tip velocity $V_{tip-2} = 1/2\Delta V_2$. The second stage, therefore, utilizes the tether more efficiently than the first stage.

After adopting cylindrical tethers, which are perfectly adequate for a two-stage tethered system, the centrifugal force at the c.m. of the ith stage is as follows:

$$F_{c.m.} = L_{i2}\omega_i^2 m_{pay} + \int_0^{L_{i2}} \rho A \omega_i^2 l \, dl$$

$$= \frac{V_{tip-i}^2}{L_{i2}} \left(m_{pay} + \frac{1}{2}\rho A L_{i2} \right), \qquad i = 1, 2 \qquad (16)$$

At the design strength of the tether $\sigma A = F_{c.m.}$ and, after recalling the definition of the tether characteristic velocity, Eq. (16) yields

$$V_c = V_{tip-i} \sqrt{(2/L_{i2})(m_{pay}/\rho A) + 1}, \qquad i = 1, 2 \qquad (17)$$

After several algebraic manipulations, Eq. (17) yields the tether-strength equation for the second stage as follows:

$$\left\{ \sqrt{\frac{\mu}{r_{p1}}} \frac{1 + \tau_2}{1 + \chi_2 + \tau_2} \left(\sqrt{2 - (1 - e_1)N^{-\frac{2}{3}}} - \sqrt{2 - (1 - e_1)M^{-\frac{2}{3}}} \right) \right\}$$

$$\times \sqrt{\frac{4(1 + \chi_2 + \tau_2)}{2 + \tau_2} \frac{\chi_2}{\tau_2} + 1} - V_c \approx 0 \qquad (18)$$

The orbital constraint for the first stage is imposed on the perigee radius of the platform after release. To prevent the platform from reentering after release of the payload, we impose a minimum perigee altitude after release r_{min}. By utilizing again the conservation of angular momentum, as expressed in Eq. (14a), we obtain the following orbital constraint equation for the first stage:

$$2\left\{ \sqrt{1 + e_1} - \frac{2\chi_1 + \tau_1}{2 + \tau_1} \left(\sqrt{2 - (1 - e_1)M^{-\frac{2}{3}}} - \sqrt{1 + e_1} \right) \right\}^{-2}$$

$$- \frac{r_{p1}}{r_{min}} - 1 \approx 0 \qquad (19)$$

and the tether-strength constraint as follows:

$$\sqrt{\frac{\mu}{r_{p1}}}\left(\sqrt{2-(1-e_1)M^{-\frac{2}{3}}}-\sqrt{1+e_1}\right)$$

$$\times\sqrt{\frac{4(1+\chi_1+\tau_1)\,\chi_1}{2+\tau_1}\frac{\chi_1}{\tau_1}+1}-V_c\approx 0 \qquad (20)$$

Equations (15) and (18–20) must be solved for different values of the orbital ratios M/N as specified by Eq. (6).

The value of orbital eccentricity e_1 of the first stage is defined by the requirement that the first stage be reachable by ground launchers. The perigee radius and the eccentricity determine the energy of the first stage orbit as $E=-\mu/(2a_1)$, where $a_1=r_{p1}/(1-e_1)$. Clearly the greater e_1 the smaller the total ΔV that the upper stage must provide to achieve GTO but also the greater the energy required to the ground launcher. Also, the smaller the perigee radius r_{p1} is the smaller the energy. However, r_{p1} must be such that the altitude of the first stage is well above the dense atmosphere. We have adopted a perigee altitude of 450 km (i.e., $r_{p1}=6828$ km) and an orbital eccentricity $e_1=0.1$ that defines an orbit of the first stage that is reachable by a number of existing launchers and likely by the presently under development RLV.

Equations (15) and (18–20) have been solved numerically for χ_1, χ_2, τ_1, and τ_2 for various orbital period ratios to determine the total mass of the system. Figure 6 shows the ratio of the total system mass (without payload) over the payload mass for ratios $M/N = 1/2$, $1/3$, and $1/4$ and M ranging from 1 to 2.2. Note that M is the ratio between the TO and LEO orbital periods whereas N is the ratio between the MEO and LEO orbital periods. The preceding equations also show that the mass ratios of the first stage are not coupled to the mass ratios of the second stage whereas the equations for the two stages are coupled through the orbital period ratios M and N.

Low total masses are obtained for $M/N =1/3$ and $M/N =1/4$. A ratio of 1/3 has two significant advantages over a ratio of 1/4 as follows: 1) the revisit time (proportional to N) is shorter and 2) the platform–2/tether–2 mass ratio (second stage) is more favorable as it allows for a bigger platform that can better accommodate subsystems and propellant.

Small values of M would appear appealing at first glance from Fig. 6, but such small values lead to a vanishing mass of the second-stage platform. Because several heavy subsystems (e.g., power) must be placed in the platform, we adopt (Fig. 7) the value $M =1.5$ that provides the highest value of the platform/payload mass ratio for the second stage. Consequently, our selection is $M =1.5$ and $N =4.5$ that also leads to a sensible mass value (Fig. 8) of the first-stage service module (platform–1).

The total mass of the system (without reboost propellant and payload) is, in conclusion, only four times the payload mass. This result is rather appealing when considering the mass of existing up-
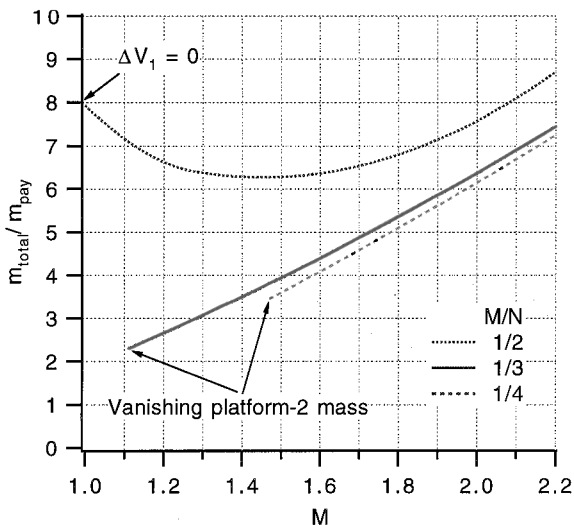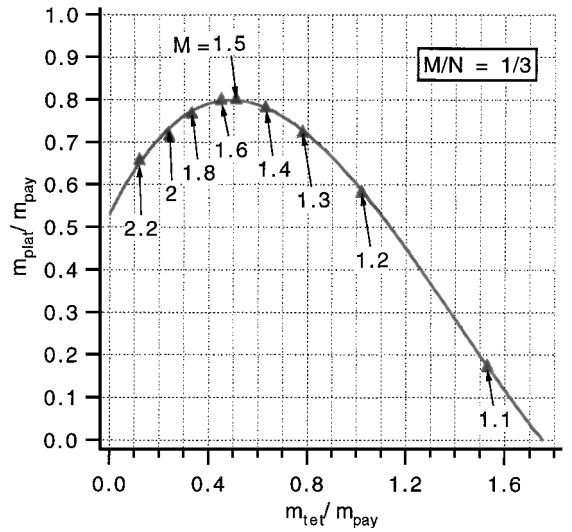

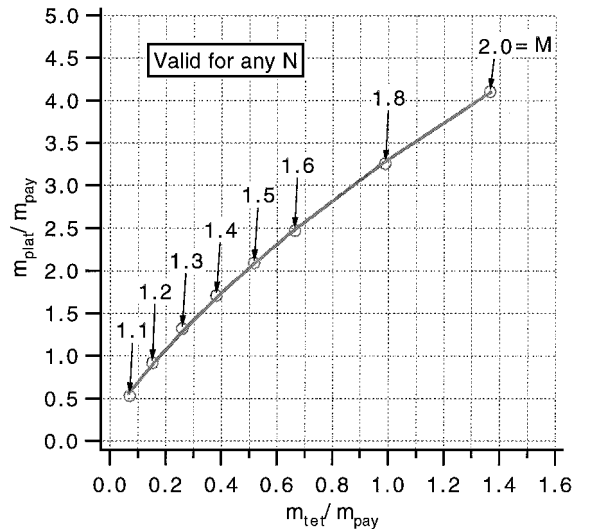**Fig. 7 Platform/payload mass ratio vs tether/payload mass ratio for second stage.**

Fig. 8 Platform/payload mass ratio vs tether/payload mass ratio for first stage.

per stages (more on this point later) and previous studies of spinning systems designed to provide a ΔV of 1.2 km/s (i.e., half the ΔV provided by the system under investigation) that resulted in system masses 30 times the payload mass.[8]

An analysis of the relevant equations also leads to the conclusion that the tether lengths play a negligible role in defining the system mass. The tether lengths, however, define the spin rates of the two stages [see Eqs. (10a) and (10b)] and, consequently, determine the acceleration at rendezvous and the acceleration acting on the payload attached to the spinning stages.

Numerical Cases

By using the equations and parameters derived in the preceding section, the orbits and other key system data have been computed, and the results are shown in Table 1. This analysis neglects the effect of air drag (which was proven to be very small in Ref. 1) and higher order gravity effects. However, the effect of the J_2 gravity term on the differential precession of the apsidal lines of the two stages can not be forgotten. This effect determines the payload transfer frequency of the two-stage system. The ideal maximum transfer frequency is equal to the realignment frequency of the apsidal lines of the stages. For the orbital design derived in this paper, the frequency of apsidal realignment (and consequently the transfer frequency) is equal to once every 72 days and, consequently, the maximum launch rate is 5 launches per year.

Fig. 6 Total/payload mass ratio for various orbital period ratios M/N.

Table 1 Key parameters of two-stage tethered system from LEO to GEO for orbital ratios $M = 1.5$ and $N = 4.5$ and single-stage tethered system

Item	Two stage	Single stage (tapered tether)
1st-stage mass ratio	$\chi_1 = 0.479$, $\tau_1 = 0.248$	$\chi_1 = 0.5$, $\tau_1 = 4.45$
2nd-stage mass ratio	$\chi_2 = 1.245$, $\tau_2 = 0.643$	N/A
LEO eccentricity	$e_1 = 0.1$	$e_1 = 0.1$
Capture revisit time, h:min	8:10	N/A
LEO–GEO transfer time, h:min	16:50	5:18
1st-stage tether length, km	$L_1 = 60$	$L_1 = 90$
2nd-stage tether length, km	$L_2 = 80$	N/A
1st-stage CM orbit		
Radii, km	$6{,}828 \times 8{,}345$	$6{,}828 \times 8{,}345$
Altitudes, km	$450 \times 1{,}967$	$450 \times 1{,}967$
2nd-stage CM orbit, km	$6{,}931 \times 34{,}426$	N/A
Payload orbit after 1st-stage release, km	$6{,}867 \times 13{,}016$	$6{,}877 \times 42{,}165$
Payload orbit after 2nd-stage release, km	$6{,}940 \times 42{,}165$	N/A
Inertial rotational rate ω_1, rad/s	0.0180	0.040
Inertial rotational rate ω_2, rad/s	0.0166	N/A
$\Delta V_1 = V_{\text{tip-1}}$, km/s	0.70	1.97
$\Delta V_2 = 2V_{\text{tip-2}}$, km/s	1.21	N/A
$\Delta V_1 + \Delta V_2$, km/s	1.91	N/A
ΔV_{circ}, km/s (not supplied by tether)	1.44	1.44
Payload acceleration on 1st-stage, g	1.0	8.1
LV acceleration at capture, g	1.8	N/A
LH acceleration at capture, g	0	N/A
Tether-1 mass, kg	2,110	36,340
Platform-1 mass, kg	8,520	8,160
1st-stage mass, kg	10,630	44,500
Tether-2 mass, kg	2,110	N/A
Platform-2 mass, kg	3,280	N/A
2nd-stage mass, kg	5,390	N/A
Mass total (at end of life), kg	16,020	44,500

Table 2 Power and propellant mass of a two-stage LEO to GEO tether system for 10 transfers over two years

Power, kW 1st stage	Propellant, kg 1st stage	Power, kW 2nd stage	Propellant, kg 2nd stage	Total propellant, kg
13	1960	22	3420	5380

Table 3 Mass of a two-stage LEO to GEO tether system for 10 transfers over two years

Dry mass, kg 1st stage	Dry mass, kg 2nd stage	Total dry mass, kg	Total propellant mass, kg	Total system mass, kg
10,630	5,390	16,020	5,380	21,400

inclusive of propellant for one launch. Consequently, the two-stage tethered system is more competitive than its chemical counterpart, on a mass basis, after two launches. Other considerations related to providing redundancies over the long operating time can increase the mass estimate of this tethered system if the system is required to be completely independent of ground servicing.

Lighter Payloads

The case shown in Tables 1 and 2 is for the heaviest payloads of 4082 kg (9000 lb). The system, however, can handle any lighter payload with ease. Lighter payloads only require adjustments of the rotational rates of the two stages and a few kilometer adjustments of the orbits to compensate for the shift of the c.m. of the two stages due to the lighter payloads.

Tether Sizes

Fail-safe tethers will likely be the preferable candidates for spinning tethers. If we assume, for the sake of picturing the size, that the tethers are cylindrical with a solid cross section, the tether diameters for the two-stage system under consideration would be 6.8 mm for the first-stage tether and 5.9 mm for the second stage.

Tether Rebound

One important issue relevant to the release of heavy payloads with long tethers is the recoil of the tether after release and the transient dynamics of the system after payload capture. The issue of tether recoil was treated in Ref. 9 where the release dynamics of heavily loaded tethers was analyzed. The solution adopted for eliminating the rebound was to generate, by reeling in and out the tether at the deployer, a tension elastic wave along the tether before payload release. The payload is, then, released when the value of the tension, produced by the tension wave at the opposite tether tip where the tether grabbing/release mechanism is located, is equal to the steady-state value of the tether tension after the payload has been released. The case analyzed in Ref. 9 was an 80-km tether, and the tension was reduced, without incurring any slackness, to 5% of its original value with a tension wave produced by reeling in and out about 500 m of tether length. Numerical simulations were utilized to prove the validity of the technique.[9] A similar strategy was utilized and simulated in Ref. 10 for reducing the transient dynamics after the capture of a payload by a spinning tether system capable of providing 1-km/s velocity increment (i.e., comparable to the velocity increments under analysis in this paper).

Transfer Time and Revisit Time

The total transfer time from LEO to GEO in case the satellite is captured at the first attempt is 16 h 50 min. The revisit time $T_{\text{rev}} = NKP_1$ between the second stage and the satellite released from the first stage in case of miscapture is equal to 8 h 10 min.

Flow of Angular Momentum

The tethered system discussed here is reversible: It can be used to transport spent satellites from GEO to LEO. In this case the second stage would capture the satellite at the top of its spin and release at the bottom of its spin to rendezvous with the first stage. Another interesting feature is that thanks to conservation of angular momentum, if a satellite is transferred to GEO and an equal-mass

The results presented in this section were derived for the heaviest payloads predicted in the traffic model, that is, telecommunication satellites of 4082 kg (9000-lb class) that are heavier than an Intelsat VII. Table 1 also shows comparable results for a single-stage, 90-km-long system that uses a tapered Spectra 2000 tether to inject the payload directly into the GTO orbit. Clearly, the launch frequency of the single stage is not determined by the realignment of apsidal lines but rather by the time required for rebuilding the total (i.e., orbital and rotational) angular momentum lost by the stage after each transfer. A few weeks are required with present technology ion thrusters for an efficient reboosting of the stage.

Power, Reboost Propellant, and System Mass

Ion thrusters with a specific impulse of 1500 s were assumed for reboosting the stages after each launch. As shown in Table 2 (see Ref. 1), 5 missions per year with the heaviest payloads and a two-year interval between propellant deliveries were also assumed to compute the power and propellant consumption. Power demand can be lowered and propellant increased by lowering the specific impulse of the thrusters. The low propellant mass required to cover 10 launches over a two-year cycle highlights one of the fundamental characteristic of this transportation system, that is, the system combines the efficiency of electrical propulsion with the delivery speed of a chemical upper stage.

The total mass of the system for 10 launches over two years of operation is 21,400 kg that is divided between 16,020 kg of empty system mass (at end of life) and 5380 kg of reboost propellant (see Table 3). A chemical upper stage with comparable payload capacity to GTO (e.g., Inertial Upper Stage) has a total mass of 14,800 kg

satellite is retrieved from GEO at the next available opportunity, no propellant is required for reboosting the stages. Clearly, in a realistic situation the return traffic will be different from the outgoing traffic, and some propellant will be necessary for making up the deficit of angular momentum and also for orbital phasing. The return traffic, besides being important in itself, can also provide sizable savings to the propellant budget of the system, which is worth further analysis.

Rendezvous and Capture

One of the important aspect of a two-stage tethered system is the capture of the satellite by the second stage. A few important points must be stressed regarding this particular rendezvous and capture as follows: 1) the relative velocity at capture is zero, 2) the horizontal component of the relative acceleration is zero, 3) the vertical component of the relative acceleration is about 1.8 g for the case analyzed, and 4) the timing of the rendezvous maneuver is faster than a conventional rendezvous.

Simulations of the rendezvous and capture phase were carried out with a simplified model that simulates the dynamics in the equatorial plane and neglects air drag and higher order gravity harmonics. The trajectory of the payload as seen from the tip of the second stage is shown in Fig. 9. The dotted line in Fig. 9 is the trajectory that the payload would follow if it is not captured by the second stage. The relative velocity and acceleration between the tip of the second stage and the incoming payload are shown in Figs. 10a and 10b.

Considering that the vertical acceleration is the only nonzero component at capture, the capture maneuver is fairly similar (except for the g value) to capturing an object, thrown in the air from the ground, at the top of its parabolic trajectory with the hand moving at the same horizontal velocity of the object. The only nonzero component at capture is, in both cases, the vertical acceleration that is equal to 1 g on the ground and 1.8 g for the tethered system under consideration. The vertical component of the relative acceleration at capture is simply $a_{max} = V_{tip}^2 / l_{22}$. Consequently, the value of the maximum relative acceleration can be reduced by utilizing a longer tether for the second stage without requiring significant changes to the rest of the system.

Orbital mismatches at capture can be compensated for by adjusting the time of payload release and the spin rate of the first stage. For example, the line of apses of the payload transfer orbit (after release from the first stage) can be rotated by changing the time of payload release during the spin. A payload release with the tether crossing the local vertical produces a ΔV with no vertical component and, therefore, no rotation of the line of apses. On the contrary, a release off the local vertical advances or retards the position of the line of apses and, consequently, can correct possible mismatches
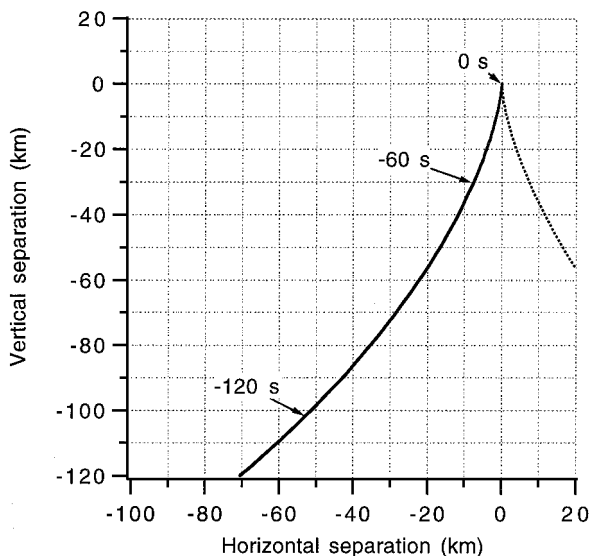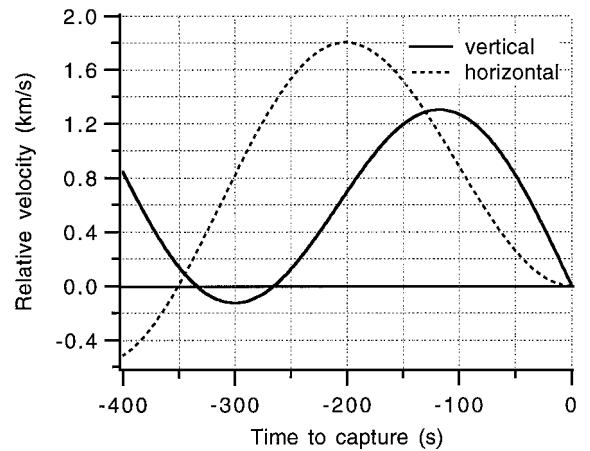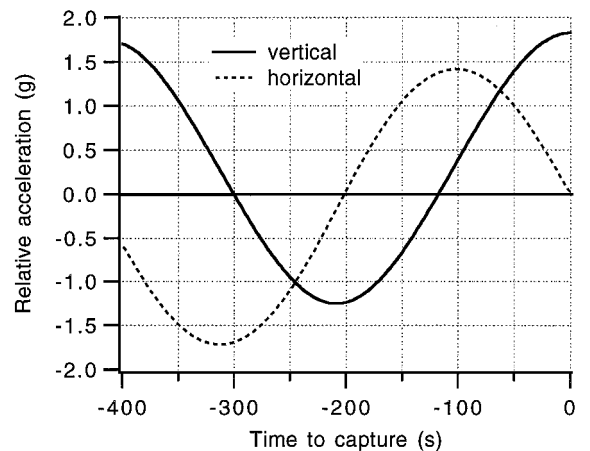
a) Relative velocity components

b) Relative acceleration components

Fig. 10   Rendezvous and capture dynamics of payload by second stage.

along the orbital track. For example, releasing the payload 5 deg before or after the local vertical rotates the lines of apses of the first stage orbit by ± 1.7 deg (a 5-deg phase shift at release corresponds to a time shift of 4.8 s for the payload release from the first stage.) A 1.7-deg rotation of the line of apses of the transfer orbit equals a 202-km along-track error of the position of the second stage at payload capture.

A radial error of the second stage at capture can be compensated for by adjusting the spin rate of the first stage. This adjustment can be done without any propellant consumption by simply changing the tether length, that is, utilizing the conservation of angular momentum. A reduction or increase of the first stage tether length of 3.1% of the full length produces a change of the transfer orbit apogee altitude of 200 km. Consequently, a radial error of 200 km can be compensated with a 1.9-km change of the first stage 60-km tether length.

A comprehensive analysis of the payload rendezvous and capture is beyond the scope of this paper. A conceptual design of the capture devise and a preliminary analysis of the sensors and actuators required for the rendezvous and capture was carried out in Ref. 1. The conclusion from that study is that the sensors and actuators requirements are within the state of the art and that given the availability of differential global positioning system navigation there are no critical impediments to this type of rendezvous. However, further analyzes are needed for a more in-depth definition of the hardware involved.

Recommendations for Further Analysis

This paper focuses on some of the critical issues related to developing a spinning tether architecture for transferring payloads from LEO to GEO. A number of key issues have also been analyzed in other references.[1,9,10] There is, however, a number of topics that are

Fig. 9   Trajectory of rendezvous and capture of payload by second stage (payload escape trajectory shown in dashed line).

recommended for further analysis as follows: 1) evaluating the influence of environmental perturbations over time and devising the necessary adjustments, 2) developing strategies for guidance and control during rendezvous and docking, 3) assessing the flow of angular momentum and the use of the return traffic to restore momentum, and 4) incorporating the techniques developed in Refs. 9 and 10 for mitigating the tether transient dynamics into the simulations of payload capture and release.

Conclusions

A spinning tethered system for transfers from LEO to GEO combines the efficiency of electrical propulsion (high specific impulse) and the delivery speed of a chemical system. A two-stage tether system of reasonable size and relatively small mass can be devised for transferring payloads with a mass up to 4000 kg to GEO with the circularization velocity increment provided by the kick motor of the payload. The transfer time for the two-stage tether system is 16 h 50 min, which is comparable to the typical 5 h 30 min transfer time of a chemical upper stage. The study shows that a two-stage tether system is more competitive, on a mass basis, than a chemical-propellant upper stage after two orbital transfers.

The orbital design of the system makes use of resonant orbits to provide periodic conjunctions (or visits) between the first and second stage and multiple opportunities for capture of the payload in case of miscapture by the second stage. The ideal transfer frequency of a two-stage system is determined by the periodic realignment (dependent on the Earth oblateness) of the two stages' apsidal lines. The ideal maximum transfer rate consistent with the orbital design derived in this paper is once every 72 days or five transfers per year. The transfer rate of a single-stage system is not determined by apsidal realignment but rather by the time required for efficiently reboosting the stage. A single-stage system is three times heavier than a two-stage system with present-day tether materials, but it should be considered in the future as tether material characteristics improve.

References

[1]Bangham, M. E., Lorenzini, E., and Vestal, L., "Tether Transport System Study," NASA TP-1998-206959, March 1998.

[2]Fuller, P. N., "Commercial Spacecraft Mission Model Update," Rept. of the COMSTAC Technology and Innovation Working Group, U.S. Dept. of Transportation, Washington, DC, July 1995.

[3]Bekey, I., and Penzo, P., "Tether Propulsion," *Aerospace America*, Vol. 24, No. 7, 1986, pp. 40–43.

[4]Carroll, J. A., "Guidebook for Analysis of Tether Applications," NASA CR-178904, March 1985.

[5]Hoyt, R. P., "Tether System for Exchanging Payloads Between the International Space Station and the Lunar Surface," Tether Technology Interchange Meeting, NASA CP-1998-206900, Jan. 1998, pp. 271–284.

[6]Moravec, H., "A Non-Synchronous Orbital Skyhook," *Journal of the Astronautical Sciences*, Vol. 25, No. 4, 1977, pp. 307–322.

[7]Puig-Suari, J., Longuski, J. M., and Tragesser, S. G., "A Tether Sling for Lunar and Interplanetary Exploration," International Academy of Astronautics, Paper IAA-L-0701P, April 1994.

[8]Oldson, J., and Carroll, J. A., "Potential Launch Cost Savings of a Tether Transport Facility," AIAA Paper 95-2895, July 1995.

[9]Colombo, G., "Orbital Transfer and Release of Tethered Payloads," NASA CR-170779, March 1983.

[10]Carroll, J. A., "Preliminary Design of a 1 km/s Tether Transport Facility," NASA Final Rept. NASW-4461, March 1991.

I. E. Vas
Associate Editor